Nonlinear behavior of photoabsorption in hexagonal nitride quantum wells due to free carrier screening of the internal fields

S. Kalliakos, P. Lefebvre, and T. Taliercio
Groupe d'Etude des Semiconducteurs, CNRS, Université Montpellier II, Case Courrier 074, 34095 Montpellier Cedex 5, France
(Received 29 April 2002; revised manuscript received 23 January 2003; published 8 May 2003)

We investigate the effects of large electron-hole pair densities on the energy spectra of quantum wells based on hexagonal group-III nitrides, such as $GaN/Al_xGa_{1-x}N$ or $In_yGa_{1-y}N/GaN$ systems. More specifically, we solve self-consistently the Schrödinger and Poisson equations in order to calculate the changes in emission and absorption spectra, induced by the screening of the large internal electric fields that are present in these systems. In particular, we find that pair densities of a few times 10^{12} cm^{-2} induce not only a blueshift of the fundamental transition but also a significant *enhancement* of the absorption coefficient, in the region corresponding to transitions between excited states. We estimate the typical optical power densities necessary to induce such effects.

DOI: 10.1103/PhysRevB.67.205307 PACS number(s): 78.67.De, 78.67.Hc, 73.21.Fg, 73.21.La

INTRODUCTION

A lot of work has been done, especially in the past two decades, to get an insight into the physical mechanisms in semiconductor low-dimensional systems such as quantum wells (QW's) or quantum boxes (QB's), particularly in order to produce new concepts of optoelectronic devices. Passive devices, based on the change of absorption coefficient with applied voltage, such as electro-optical modulators and bistable switches, have received a great attention. While for three-dimensional semiconductors the mechanism responsible for the modulation is the Franz-Keldysh effect,[1,2] for QW's, it is the quantum-confined Stark effect (QCSE).[3,4] In addition, interesting effects occur under high-carrier-injection conditions and their interpretation is crucial, not only for the operation of the passive devices, but also for active ones, especially light-emitting devices. Among others, we should mention the bleaching of the excitonic properties,[5] the band-gap renormalization,[6,7] and the screening of an externally applied electric field.[8] More specifically, several early works[9–12] have emphasized nonlinear optical properties that can result from the screening of internal piezoelectric fields that are present in (Ga,In,As)-based quantum wells or superlattices by photoinjection of high densities of electron-hole (*e*-*h*) pairs.

In recent years, a lot of attention has been paid to a new class of low-dimensional structures, made of hexagonal (wurtzite) group-III nitride semiconductors, due to their potential application as the active materials for short-wavelength laser emission.[13] The main peculiarity of these systems is the existence of an internal electric field comparable to or much larger than 1 MV/cm, along the growth axis. The origin of this large electric field[14–16] is the difference in both the spontaneous and piezoelectric polarizations between the barrier and well materials. This electric field strongly modifies the optical properties of the QW's or QB's. First, it induces a large redshift in the transition energies, because of the QCSE,[17–22] such that the emission of the QW can cover the entire visible spectrum[20–22] by changing the well width, although the band gap of the well material corresponds to ultraviolet photon energies. Second, this field separates the electron and hole wave functions towards the opposite sides of the well. This drastically decreases the oscillator strength of the fundamental transition and hence increases the radiative recombination time[17,20,23,24] with a nearly exponential dependence with well width. It is important to emphasize that QB's made of hexagonal group-III nitrides have also been produced[21,22,25] and that they obey exactly the same rules concerning the QCSE. This is mainly due to the small exciton Bohr radius in these materials ($\sim$3 nm), which is, in most cases, smaller than the in-plane size of the boxes. In other words, lateral confinement effects are quite negligible, and the general properties of absorption or emission of such QB's are comparable to those of QW's of similar vertical sizes. Nevertheless, the growth of QB's is a way to block the in-plane motion of carriers, thus reducing the probability of *nonradiative* recombinations. The latter mainly correspond to the capture of carriers at defects such as threading dislocations, and they may become dominant when the temperature of the sample is raised to 300 K. In fact, any kind of short-range localization, like that which occurs naturally in the disordered ternary alloy $In_yGa_{1-y}N$, is beneficial in terms of enhancement of the nonradiative lifetime.[25] To this extent, group-III nitrides are particularly advantageous too, because they can easily produce band-gap differences of the order of 1 eV or more, and thus induce efficient confinement. This effect is further enhanced by very large effective masses ($0.2m_0$ for electrons and larger than $1m_0$ for holes), which also dramatically increases the densities of states in two-dimensional (2D) systems if compared to more familiar QW's such as $GaAs/Al_xGa_{1-x}As$ and $In_yGa_{1-y}As/GaAs$.

Considering the ''giant''confinement, Stark effect, and densities of states, the purpose of this work is to predict, by using envelope-function calculations, some original phenomena that should be observable in group-III nitride QW's (or planes of QB's) under high photoexcitation conditions. Given the current uncertainty on several physical parameters, starting with the electric field itself, our aim is not to give accurate prescriptions for active device systems. Instead, we

will provide a qualitative description of the physical processes at work and emphasize the advantages of group-III nitrides.

A number of interesting effects have already been predicted and/or experimentally verified, such as the screening of the excitonic interaction.[26] We will specifically investigate the screening of the internal electric field in the well[6,9–12] that can lead (among others) to (1) a blueshift of the emission spectrum due to the partial cancellation of the QCSE,[27–30] (2) a higher recombination rate for the optical transitions,[29–33] (3) a modification in the absorption spectrum[34,35] due to the direct relation of the absorption coefficient with the oscillator strength, and (4) an influence on the optical gain properties of $In_yGa_{1-y}N$/GaN-based lasers.[36] The oscillator strength is proportional to the square overlap integral of the electron and hole envelope functions (hereafter referred to as the ''overlap integral''). For the ground-state transition ($E1$-$H1$) in nitride-based heterostructures, this quantity can be very small due to the spatial separation of electrons and holes. We must consider, too, that large *e-h* pair densities can induce a significant band-gap renormalization, due to many-body effects.[35,37,38] The main effect of this renormalization is an overall redshift of all transition energies. To the best of our knowledge, the most complete attempt of theoretical description of the high photoexcitation of nitride QW's is that of Ref. 35, including the screening of excitonic effects, the screening of the internal field, many-body effects, and valence-band mixing. However, *all* of the above-mentioned works were restricted to the spectral region near the ground-state transition ($E1$-$H1$).

In this work, contrary to previous ones, we calculate the entire interband absorption spectrum of $GaN/Al_xGa_{1-x}N$ QW's, thus including excited states, and we investigate its change under high photoexcitation. We find that a significant positive differential absorption (PDA) can be induced in these structures, and we estimate the optical power densities necessary to produce such a nonlinear optical effect.

THEORETICAL MODEL

To calculate the effect of high densities of *e-h* pairs, we solve self-consistently the Schrödinger and Poisson equations within the envelope function approximation. We only consider the first three confined subbands for electrons and the first six subbands for ''heavy'' and ''light'' holes. In fact, the valence band of wurtzite nitrides is threefold, with the maxima of the so-called *A* (''heavy holes,'' *H*), *B* (light holes, *L*), and *C* bands lying within a few tens of meV.

In the majority of cases, the nitride-based QW's and QB's are made of GaN or $In_yGa_{1-y}N$ layers that are under biaxial elastic compression because of the lattice mismatch with the barrier material, itself strained by a buffer layer, usually made of GaN. For samples grown on sapphire substrates (most of the cases), it is well-known[39,40] that this buffer always undergoes some degree of in-plane biaxial compression. The biaxial compression of the well (or box), the ''crystal field'' induced by the hexagonal symmetry, and the spin-orbit coupling have an intricate effect on the structure of the valence band, but the result is rather simple. Figure 1 shows

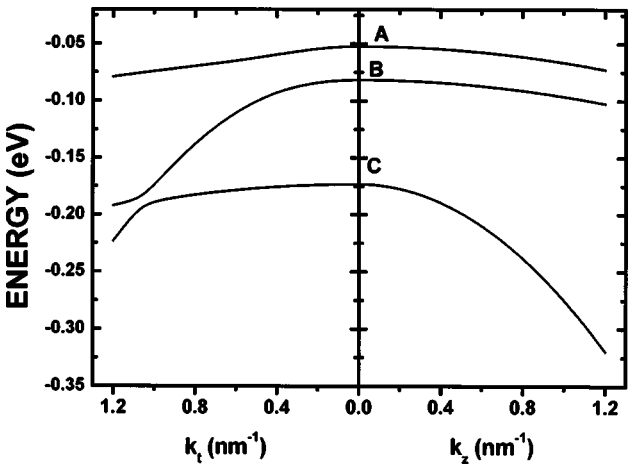

FIG. 1. Calculated valence bands of a GaN epilayer, with a biaxial in-plane compression perpendicular to the (0001) direction (the *z* axis). The quasicubic approximation was used, identifying the (0001) direction of the wurtzite structure with the (111) direction of the zinc-blende structure. For the in-plane dispersion curves, we have used $k_t=(k_x^2+k_y^2)^{1/2}$. The numerical parameters used are gathered in Table I.

the dispersion relations for GaN, calculated using the parameters gathered in Table I, including some typical in-plane biaxial compression δ. The *A* and *B* bands have nearly parallel dispersion relations along the *z* direction, i.e., the (0001) growth axis. Consequently, the effective masses for the *A* and *B* bands along this axis are quite similar (and quite large). We take the same value of $m_A=m_B=1.1m_0$, for GaN (Ref. 42). As a result for a given QW, each heavy-hole subband is accompanied by a light-hole companion at a constant distance that is fixed by the splitting of the *A* and *B* bands in the strained GaN, i.e., ~30 meV, from our calculations. On the other hand, the effective mass for the *C* band is much smaller ($m_C=0.15m_0$, Ref. 42) and thus, for narrow QW's such as those considered here, there are only few confined

TABLE I. The valence-band parameters used in our calculation of the dispersion relation of GaN (Fig. 1).

A_1	-6.56[a]
A_2	-0.91[a]
A_3	-5.65[a]
A_4	-2.83[a]
A_5	-3.13[a]
D_1 (eV)	-5.32[b]
D_2 (eV)	-10.23[b]
D_3 (eV)	-4.91[b]
D_4 (eV)	2.7[b]
Δ_1 (eV)	0.022[c]
Δ_2 (eV)	0.015[c]
Δ_3 (eV)	0.005[c]
δ	-0.01

[a]Reference 42.
[b]Reference 39.
[c]Reference 41.

levels, and they are pushed to much higher energies than those arising from the *A* and *B* bands.

Concerning the oscillator strengths of the various interband optical transitions, probed by transmission experiments, we consider only the case of normal incidence, i.e., with the light polarized along the growth plane. In this case, the dipole matrix element between the valence band and conduction band is nonvanishing for both the *A* and *B* states, whereas it is close to zero for the states of the *C* band. It has been shown,[39,40,43,44] moreover, that due to the biaxial compression, the optical matrix elements are nearly equal for the *A* and *B* transitions. We thus assume equivalent oscillator strengths for both *A*- and *B*-related valence subbands, and we do not include the *C*-hole states in the calculations.

Moreover, we do not include excitonic properties, since it has been established earlier[26] that the exciton binding energy goes to zero for carrier densities of a few 10^{11} cm^{-2}, lower by one order of magnitude than those considered in this work. Assuming continuous-wave excitation conditions, we model a quasiequilibrium situation, leading to a given steady-state density of *e-h* pairs. Using the two-dimensional densities of states, proportional to the appropriate in-plane effective masses, we calculate the population of each subband and the quasi-Fermi-levels for electrons and holes. Given the population of each subband, we calculate the modification of the potential by solving Poisson's equation:

$$\frac{d^2V_{\mathrm{Pois}}}{dz^2} = -\frac{\rho(z)}{\varepsilon\varepsilon_0}, \tag{1}$$

where $\rho(z)$ is the charge density profile given by

$$\rho(z) = e\sum_{i,j}\,[n_{hi}|f_{hi}(z)|^2 - n_{ej}|f_{ej}(z)|^2], \tag{2}$$

where $f_{e,h,i,j}(z)$ are the envelope functions for the electrons and holes in the well and $n_{e,h,i,j}$ are the carrier populations for each subband *i* and *j*. Moreover,

$$n = \sum_{i=1}^{12} n_{hi} = \sum_{j=1}^{3} n_{ej}, \tag{3}$$

where *n* is the total density of *e-h* pairs. By using Eqs. (2) and (3), we account for the fact that the charge distribution in the QW is affected by the population of excited states and not only of the ground state. The energy levels and envelope functions are determined by slicing the space into thin layers and by using a finite-element technique. This method is more accurate than the perturbative approach, based on the mixing of the solutions of a zero-field problem,[35] which should not be used, in principle, for such large electric fields and large well widths.[45] Indeed, this approach is only valid if the Stark shift of the ground state is much smaller than the zero-field separation between $E1$ and $E2$ states,[45] which is not the case for nitride QW's. With our method, on the other hand, the details of the band curvature induced by the charge accumulation are obtained self-consistently, leaving us with a curved potential profile. This is more accurate, especially concerning the oscillator strength, than including an artificial "screening field,"[35] thus keeping a triangular band profile.

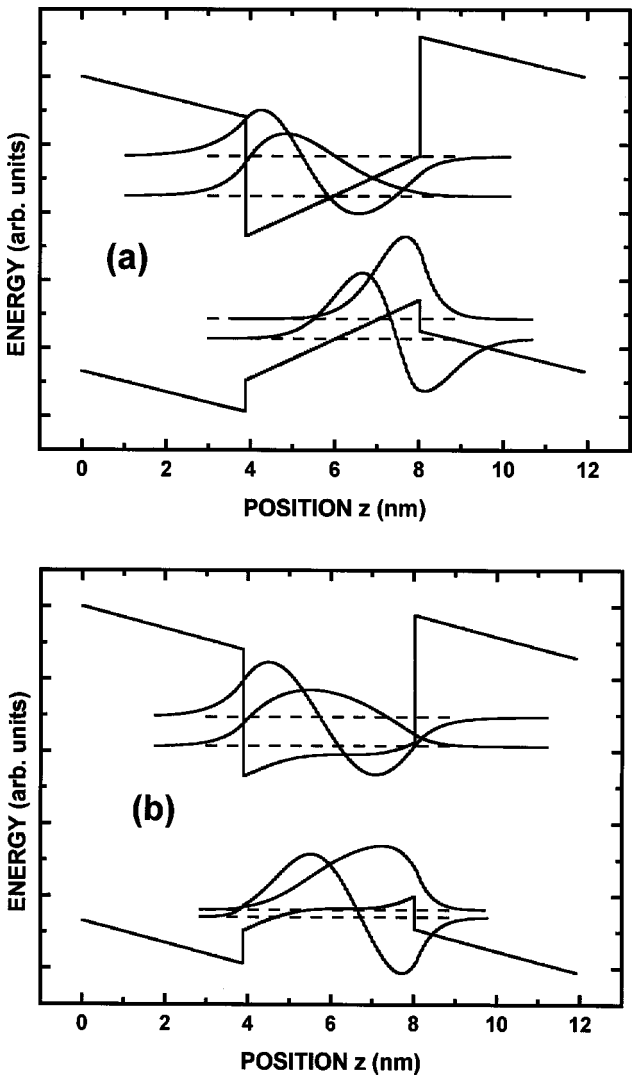

FIG. 2. The band profile of a 16-ML-wide GaN/$Al_{0.4}Ga_{0.6}N$ quantum well with opposite electric fields of $F_W = 1.4$ MV/cm and $F_B = -0.77$ MV/cm in the well and barriers, respectively. Dashed lines show the first two quantized subband minima for electrons and holes. The corresponding envelope functions are shown, too. Case (a) corresponds to the low-excitation regime, with no screening effect. Case (b) corresponds to the result of our self-consistent calculation for an electron-hole pair density $n = 6\times10^{12}$ cm^{-2}.

Figure 2 illustrates the change of the band profile of the first two quantized energy levels and of the envelope functions when large densities of pairs are present in the QW. The high excitation totally changes the splitting between the various levels and the details of the corresponding wave functions.

To calculate the interband absorption spectrum, we refer to the formulation of Haug and Koch:[46] the absorption coefficient of an ideal medium of dimensionality *d* is the product of a dimensionless spectral term and an amplitude factor. For free-carrier absorption (no excitonic effect), the spectral term follows a square-root variation with photon energy *E* for $d = 3$, whereas it is made of the addition of step functions starting at each interband transition energy E_{ij} for $d = 2$. The amplitude factors can generally be written $\alpha_0^{3D} = \Theta/(\pi a_B)$ and $\alpha_0^{2D} = \Theta/L$, where

$$\Theta = \frac{2\pi |d_{cv}|^2}{\hbar n_b c a_B^2} \tag{4}$$

is essentially the optical density of the 2D medium when probed by light propagating perpendicular to its plane. The background refractive index is n_b, and a_B is the exciton Bohr radius (3 nm for GaN), while d_{cv} is the interband optical matrix element between valence- and conduction-band Bloch states. In practice, we deal with the optical density of a quantum well, for which each interband transition (i,j) has a different oscillator strength. We thus multiply Θ by the square overlap integral of electron and hole envelope functions, $|I_{eh}(i,j)|^2$, for each steplike absorption onset. For practical reasons, we use the absorption coefficient of GaN (10^5 cm^{-1}) as a reference.[47] This coefficient corresponds to the *excitonic absorption* thus influenced by the so-called Sommerfeld enhancement factor, which is exactly equal to 2π at the band gap ($d=3$). Therefore, we have $2\pi\alpha_0^{3D} = 10^5$ cm^{-1} from which we deduce $\Theta = 1.5\times 10^{-2}$.

To account for high excitations, we increase the density of *e-h* pairs step by step, in order to describe correctly the change in energy levels in the corresponding densities of states and in overlap integrals. In addition, due to exclusion effects, such high excitations induce the bleaching of some optical transitions involving occupied final states. We account for this by multiplying the proper absorption steps by another steplike factor, i.e., zero for occupied states and 1 for the unoccupied ones, which corresponds to $T=0$ K. Finally, optical gain is also made possible for transitions between populated electron bands and populated hole bands.[35] The gain is given by the calculated absorption coefficient, with opposite sign.

To provide a more realistic picture of systems with inhomogeneous broadening, we make a convolution of the calculated spectrum by a sigmoidal function, $S(E)=(1+e^{E_{ij}-E/\Delta E})^{-1}$, where E_{ij} is the energy for each transition with a broadening factor of $\Delta E = 50$ meV. This is reasonable, considering the state-of-the art broadening of optical features and the high degree of excitation. This broadening is quite larger than the light- to-heavy-hole splitting that we calculate, and it is larger too than the splitting that one would obtain from a more tedious treatment of the valence band.

In fact, it is clear that a full treatment of the so-called ''valence-band mixings'' would improve the accuracy of theoretical predictions.[44] Nevertheless, we propose our parabolic model as a first approach to the problem to be refined in later investigations provided that the pertinent material parameters are known with accuracy (which is certainly not the case now). Although this does not constitute a proof of validity, we just wish to present the following arguments in favor of the our simplified model. Inclusion of valence-band mixings will essentially (1) change the shape of our steplike joint densities of states into more complex curves and (2) induce exchanges of oscillator strengths between anticrossing subbands. Now, regarding these oscillator strengths, we have already noticed that they were made nearly equal for heavy-hole and light-hole states by the in-plane compressive strain, and made vanishingly small for *C* holes. This makes a very large difference with more familiar systems based on zinc-blende semiconductors, where the oscillator strength of light- and heavy-hole excitons differ by a factor of 3, under normal incidence of light. Thus for the present group-III nitrides, any exchange of the ''heavy-hole'' and ''light-hole'' characteristics between two anticrossing subbands should keep the oscillator strength constant. As for the shapes of the densities of states, we consider that the broadening parameter that we chose should somehow dampen this effect, although this will have to be proven in future work.

In the following, we consider sheet carrier densities larger than the Mott density, i.e., of a few times 10^{12} cm^{-2}. In order to include the band-gap renormalization that results from carrier-carrier scattering (many-body) effects, we refer to previous works[35,37,38] where this effect has been calculated for group-III nitride-based QW's, including or not the electric field effects and/or the valence-band mixings. The main result and the only effect that previous workers have considered so far are quite simple: given a density of *e-h* pairs, the band-gap renormalization yields an overall redshift of all optical transitions. In fact, the authors of Refs. 37 and 38 have established that this redshift follows some ''universal'' behavior for nitride QW's, illustrated by Fig. 4 of Ref. 37, although electric fields were not included in Ref. 37. We have checked from the calculation of the band-gap renormalization in Ref. 38, which includes the electric field effect for a GaN/$Al_{0.2}Ga_{0.8}N$ QW, that this calculation follows the same general behavior. Then, the band-gap renormalization can be deduced from the following law, which fits the results of Ref. 37:

$$\frac{\Delta E_G}{R_{2D}} = -1.67(r_{2D})^{-0.71}, \tag{5}$$

where R_{2D} is the binding energy of two-dimensional excitons, i.e., four times the three-dimensional value for GaN ($R_{2D}=0.1$ eV) and r_{2D} the so-called ''dimensionless interparticle distance,'' which is deduced from the exciton two-dimensional Bohr radius, $a_B^{2D}=0.5a_B^{3D}$, by $r_{2D} = 1/[\pi n (a_B^{2D})^2]^{1/2}$, where $a_B^{2D}=1.5$ nm for GaN.

We estimate redshifts of 0.083 eV for $n=2\times 10^{12}$ cm^{-2} and of 0.136 eV for $n=8\times 10^{12}$ cm^{-2}. The absorption spectra calculated below do include these slight redshifts, but we insist on the following: these many-body effects cannot change the fact that the oscillator strengths of some optical transitions, especially those involving excited states, are modified by a high injection of *e-h* pairs, via the only screening of the internal electric field.

As for the dynamical aspects of the problem, we use the following equation for the injected *e-h* pair density *n*:

$$n = g\tau, \tag{6}$$

where g is the generation rate for the pairs and τ is their recombination time. The latter is given by $\tau^{-1}=\tau_R^{-1}+\tau_{NR}^{-1}$, where τ_R and τ_{NR} are the radiative and nonradiative recombination times. For low-temperature experiments or, for higher temperatures, in case of localized carriers, as for quantum boxes and/or $In_yGa_{1-y}N$ alloys (see above), the overall decay time is nearly equal to τ_R because $\tau_R \ll \tau_{NR}$. For free excitons, the nonradiative contribution may be

dominant, especially at room temperature. In the latter case, τ_{NR} is small and we will assume it independent of the *e-h* pair density. On the other hand, if the radiative recombination dominates, as the electric field is screened, the overlap integrals for the various transitions change. This contributes to the reduction of the radiative lifetime, τ_R for the $E1$-$H1$ recombination, which we calculate self-consistently. However, for densities of pairs, n, larger than the Mott density $n_{Mott}=1/(\pi a_B^2)$, where a_B is the *actual* exciton Bohr radius, we need to consider the bimolecular recombination of electrons and holes, where the recombination rate is no longer proportional to n, but proportional to n^2. We can put this in another way by considering a decay time inversely proportional to n. Eventually, we can obtain a reasonable estimation of the radiative decay time, provided that the low-excitation value $\tau(0)$ is known, as well as the change of the electron-hole square overlap integral $I_{eh}^2(n)$ by using the following approximation:

$$\frac{\tau(n)}{\tau(0)}=\begin{cases} I_{eh}^2(0)/I_{eh}^2(n) & \text{for } n<n_{Mott} \quad (7a) \\ [I_{eh}^2(0)/I_{eh}^2(n)]n_{Mott}/n & \text{for } n>n_{Mott}. \quad (7b) \end{cases}$$

The generation rate is given by

$$g=(1-e^{-\theta(E)})\frac{P_{in}}{SE}, \quad (8)$$

where $\theta(E)$ is the optical density at excitation energy E and P_{in}/S is the incident power density. Possible reflection of the incident beam is not taken into account. However, the translational asymmetry of the well makes optical transitions involving excited states more or less allowed, a situation that evolves as the system is more and more excited and that we also account for self-consistently.

RESULTS AND DISCUSSION

We present results obtained for a GaN/$Al_{0.4}Ga_{0.6}N$ QW with a width of $L_w=16$ atomic monolayers (ML's), i.e., 4.1 nm and barriers of $L_B=30$ ML. By a simple scaling procedure, based on previous experimental studies of such systems,[48,49] we can estimate the electric field and the radiative lifetime in the low-excitation regime for this QW. The fields in the well and barrier, expressed in MV/cm, are given by $F_W=5.5x\ L_B/(L_W+L_B)$ and $F_W=5.5x\ L_W/(L_W+L_B)$, where x is the Al composition in the barriers. Here, we obtain $F_W=1.4$ MV/cm and $F_B=-0.77$ MV/cm. By the appropriate calculations of overlap integrals, we can extrapolate the radiative lifetimes measured in Ref. 49, and we obtain $\tau(0)=22.2$ ns for the present example. We have taken the numerical parameters gathered in Table II for the GaN and AlN binary compounds considered near $T=0$ K. The band gap of the ternary alloy was estimated by linear-interpolation for simplicity, and we assumed a strain-free conduction-band offset of 80% of the total gap difference.

We have also performed a variational calculation of the exciton binding energy and Bohr radius; we obtain $R=24$ meV and $a_B=4.8$ nm, respectively. The binding energy is comparable to the bulk value (25 meV) because the separation of the electron and hole envelope functions by the electric field counteracts the quantum confinement. Then, we obtain $n_{Mott}\sim 1.4\times 10^{12}$ cm^{-2}.

TABLE II. The numerical parameters used in our numerical calculations of transition energies and oscillator strengths. Superscript 2D indicates the in-plane effective masses, useful for calculating the two-dimensional densities of states.

	GaN	AlN
E_g (eV)	3.5[a]	6.2[e]
E	9.5[b]	
m_e^z/m_0	0.2[c]	0.33[d]
m_e^{2D}/m_0	0.2[b]	
m_{hh}^z/m_0	1.1[e]	3.53[d]
m_{hh}^{2D}/m_0	1.65[d]	
m_{lh}^{2D}/m_0	0.15[d]	

[a]Reference 50.
[b]Reference 51.
[c]Reference 52.
[d]Reference 42.
[e]Reference 53.

Figure 3 shows the different effects contributing to the absorption onset involving the $E1$ and $H1$ subbands: the blueshifts induced by the screening of the electric field and by the filling of the subbands and the redshift induced by band-gap renormalization. For the sake of generality, we have performed the same calculations for the 4-nm-wide (Ga,In)N/GaN quantum well of Ref. 35, although it was difficult to rebuild the hole effective masses from their valence-band parameters and although their piezoelectric field is larger than 3 MV/cm, i.e., much larger than those measured experimentally. The absorption spectra of Ref. 35 include sharp excitonic resonances for $n=2\times 10^{12}$ cm^{-2} and above, which we find surprising because our own variational calculation, using their parameters, yields a binding energy of 17 meV, a Bohr radius of 4 nm, and thus a Mott density of

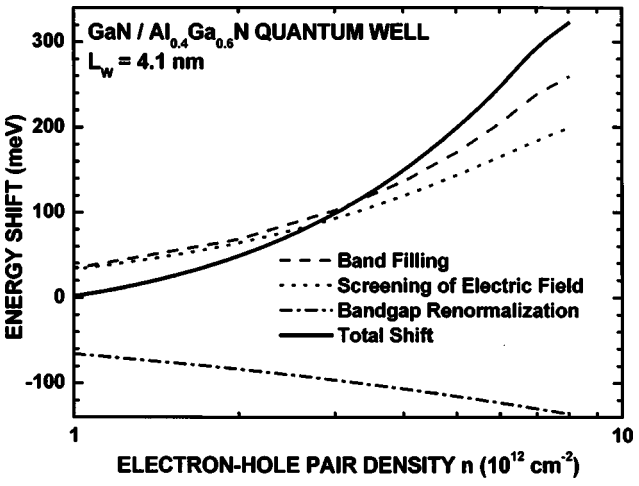

FIG. 3. The various contributions to the shift of the absorption onset for the $E1$-$H1$ transition, for a 16-ML-wide GaN/$Al_{0.4}Ga_{0.6}N$ quantum well.

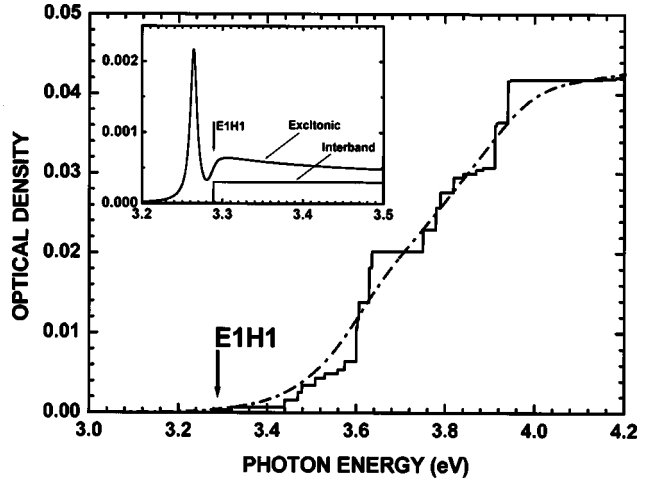

FIG. 4. The solid line shows the calculated steplike absorption spectrum for a 16-ML-wide GaN/$Al_{0.4}Ga_{0.6}N$ quantum well. Each step corresponds to a new transition energy E_{ij}. The fundamental transition $E1$-$H1$ is shown to illustrate its very small probability. The dashed curve shows the effect of the broadening. The inset shows the absorption spectrum restricted to the only fundamental ($E1$-$H1$) absorption onset, both in the interband model that we used in this work and in the excitonic approach, for a comparison with previous modelings (e.g., Ref. 35).

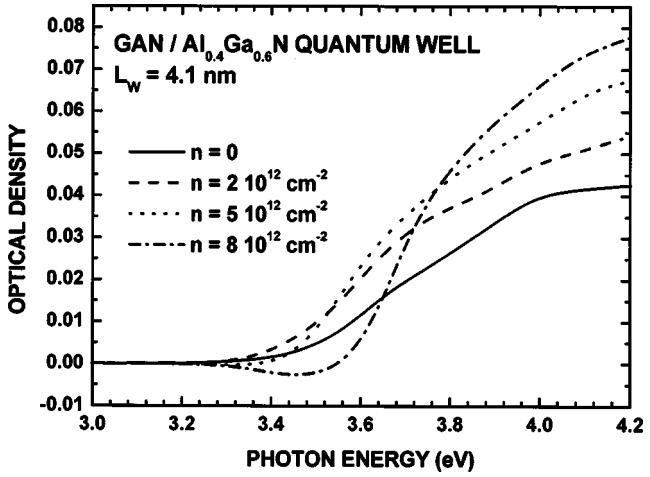

FIG. 5. Optical density spectra for a 16-ML-wide GaN-$Al_{0.4}Ga_{0.6}N$ single QW, for densities of electron-hole pairs $n=0$ (solid line), 2×10^{12} cm^{-2} (dashed line), 5×10^{12} cm^{-2} (dotted line), and 8×10^{12} cm^{-2} (dash-dotted line).

1.9×10^{12} cm^{-2}. Nevertheless, we did this comparison in order to test our simplified model against the most thorough description available. For $n=5\times10^{12}$ cm^{-2}, our calculation gives a blueshift of the absorption onset of 0.3 eV, whereas the calculation of Ref. 35 gives $\sim$0.2 eV. Considering the basic differences, commented above, between the two models, especially our more detailed description of the potential profile and envelope functions, we believe that this difference is reasonably small. We also believe that this small difference absolutely does not challenge our results on the positive differential absorption, shown below.

Figure 4 shows the optical density spectrum without and with the sigmoidal broadening function. The latter essentially smooths the steplike absorption onsets corresponding to the transitions involving the various excited states. The consideration of those states is really what makes our approach different from previous ones. To illustrate this point, the inset in Fig. 4 shows an enhanced calculated spectrum where we have only considered the fundamental transition, $E1$-$H1$, thus a single step of density of states, similar to the calculation of Ref. 35. For a better—though still qualitative—comparison with Ref. 35, we have added a calculation of the excitonic absorption with a small (and unrealistic) broadening parameter. We have used the 2D model of Shinada and Sugano,[54] including the above-mentioned exciton binding energy that we calculated. In fact, for a reasonable treatment, dimensionality issues[55,56] demand consideration, here, which is not the purpose of this paper because the present excitons have similarities with type-II excitons due to electric fields. Again, it is difficult to make an accurate comparison since we cannot know from Ref. 35 what the exciton dimensionality is. In both the present calculation and that in Ref. 35, the sharp absorption edges are simply due to the choice of a small broadening. At higher energies, the absorption spectra tends to flatten, as a result of the conjunction of the so-called Sommerfeld factor and of the 2D density of states. Now, when we properly include the excited transitions E_i-H_j and some broadening, we observe a nearly continuous increase of the absorption, reaching values that can be larger by 2 orders of magnitude than the absorption at the fundamental transition. Indeed, the latter is made extremely small by the electric-field-induced separation of electron and hole wave functions, with absorption coefficients of a few times 10^2 cm^{-1}.[35]

Figure 5 shows the optical density spectrum for four different densities of injected *e-h* pairs. The blueshift of this transition, which is the most straightforward effect of the screening of the electric field by reduction of the QCSE, is partly compensated for the lower values of n by band-gap renormalization. Several competitive mechanisms contribute to the modifications of the optical density spectrum. First, the classical bleaching of several optical transitions by population of the lower subbands tends to induce a negative differential absorption (NDA), specially in the low-energy region of the spectrum. Second, the screening of the electric field induces a blueshift of the $E1$-$H1$ transition and a significant enhancement of the absorption involving some excited states. If the band-gap renormalization (the third effect) is not included, this screening induces a positive differential absorption (PDA), only for energies larger than $\sim$3.6 eV. But the band-gap renormalization redshifts the entire absorption spectrum. The result is that (i) this PDA exists for a wider spectral region (all energies above 3.3 eV), and (ii) the amplitude of the PDA is enhanced, compared to the case where the renormalization is not included. Finally, when the pair density exceeds some $\sim5\times10^{12}$ cm^{-2}, the appearance of gain (negative absorption) increases drastically the NDA on the low-energy part of the spectrum.

More precisely, between 3.4 and 3.6 eV, when n is increased, the system starts with a PDA, but population effects suddenly reduce again the absorption coefficient above some

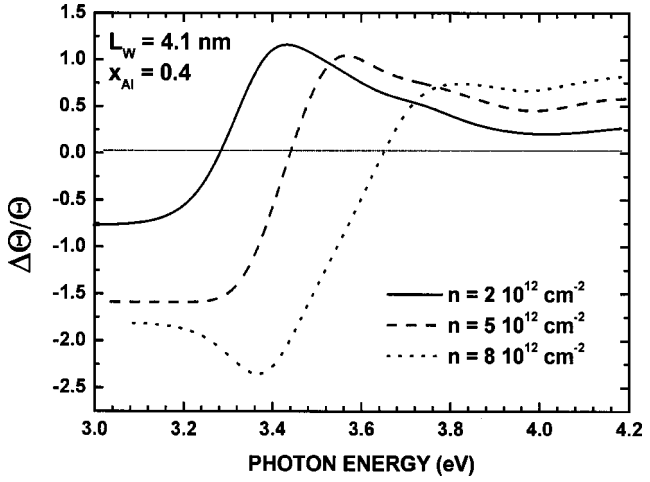

FIG. 6. Relative change of the optical density spectrum for a 16-ML-wide GaN-$Al_{0.4}Ga_{0.6}N$ single QW, between the situation where the internal electric field is not screened and cases with three different steady-state densities of electron-hole pairs, indicated in the figure.

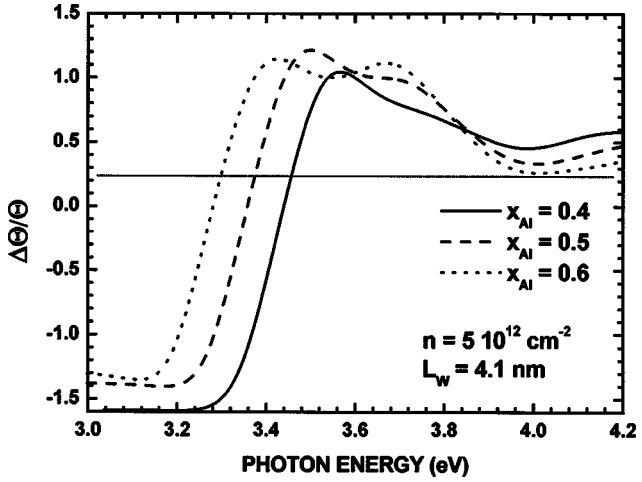

FIG. 8. The analog of Fig. 6, but for three different Al compositions, x_{Al}, in the barriers, respectively: 0.4 (straight line), 0.6 (dashed line), and 0.8 (dotted line). The injected carrier density is $n=5\times10^{12}$ cm^{-2}.

critical *e-h* pair density. This is better illustrated by the relative change of optical density, $\Delta\Theta/\Theta$ (Fig. 6), for different values of n. For instance, near 3.5 eV, the absorption coefficient is multiplied by ~ 2, for $n=5\times10^{12}$ cm^{-2} and then it collapses near zero due to band filling and gain for $n=8\times10^{12}$ cm^{-2}.

In Fig. 7, we plot the relative change in the optical density between the low-excitation conditions and that with $n=6\times10^{12}$ cm^{-2} for different well widths. We observe a larger PDA as the well width is increased, together with a redshift of the onset between zones of negative and positive differential absorption. This redshift is of ~ 0.12 eV when the well width is increased by only 4 ML, i.e., ~ 1 nm. In Fig. 8, we examine the behavior of systems with the same well width (16 ML) but with different Al compositions in the barriers for the same $n=5\times10^{12}$ cm^{-2}. As the Al composition increases, not only the barrier height but also the electric field in the well drastically increases (see above), pushing the electrons and holes apart. Consequently, the overlap integral decreases, reducing the absorption coefficient and redshifting the position of maximum PDA. In fact, Figs. 7 and 8 demonstrate the great versatility of hexagonal group-III nitride QW's and QB's, concerning these properties of differential absorption. The electric fields can be varied over a very large range from a few hundred kV/cm (Refs. 48, 49, and 53) to ~ 2.5 MV/cm for $In_{0.2}Ga_{0.8}N$/GaN QW's and QB's (Refs. 20 and 25) or even 7 MV/cm for GaN/AlN QB's.[21,22] Then the decay times can be varied[17,19,20,25] from nanoseconds (or less) to hundreds of microseconds (at least): according to Eq. (6), this provides a large versatility of the optical power densities necessary to produce these nonlinear effects (see below).

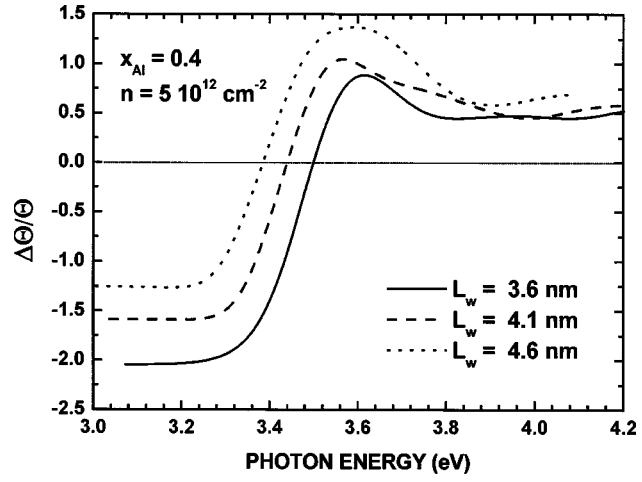

FIG. 7. Relative change of the optical density spectrum of GaN-$Al_{0.4}Ga_{0.6}N$ single QW's, for an injected electron-hole pair density of $n=6\times10^{12}$ cm^{-2}, and for respective well widths of 14 (solid line), 16 (dashed line), and 18 ML (dotted line).

In addition, group-III nitrides allow us to cover wavelengths a large part of the visible spectrum. This is due, first, to the band gaps of InN (~ 0.8 eV, from Ref. 57), of GaN (~ 3.4 eV at room temperature, from Ref. 58), and of AlN (~ 6.2 eV, from Ref. 59). But this is mostly a consequence of the giant QCSE that can push emission energies below 2 eV, whereas the band gap of the well material is close to 3 eV (ultraviolet). We thus see that the original properties discussed here can be, *a priori*, adapted to any useful spectral range, simply by changing the well width by only a few monolayers and by controlling the compositions.

This adaptability is a unique property of nitride-based low-dimensional systems: the giant Stark shift, together with large densities of states, allows electrons and holes to accumulate in a narrow spectral region, strongly redshifted from the absorption onset, which involves excited states. Then the PDA at high energies cannot be canceled by the population effects (bleaching) as it would be the case for systems such as cubic $In_yGa_{1-y}As$/GaAs QW's grown along the (111) direction, where the electric fields are smaller by one order of magnitude, the densities of states are smaller by a factor of ~ 3, and the band offsets are smaller too.[6,9–12] We also find

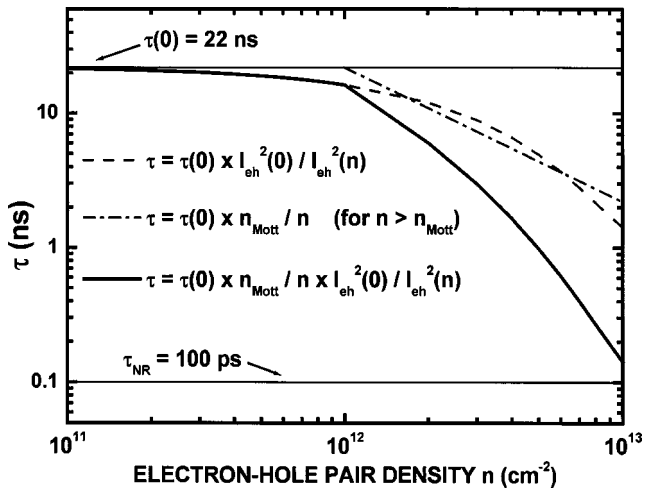

FIG. 9. Top of figure: The various contributions to the change of radiative decay time versus n, for a 16-ML-wide $GaN/Al_{0.4}Ga_{0.6}N$-quantum well. The dashed line shows the effect of increasing the oscillator strength of the $E1$-$H1$ recombination, due to the screening of the electric field. The dash-dotted line shows an estimate of the change induced by the transition from an exciton recombination regime to the bimolecular recombination of a dense population of electrons and holes. The thick solid line shows the overall result. Bottom of figure: In the case of electron-hole recombination dominated by nonradiative processes, we have assumed a constant lifetime of 100 ps.

that the redshift induced by many-body effects contributes to the enhancement of the PDA.

It is important to estimate the optical power densities required to observe these differential absorption properties. Figure 9 shows the dependence of the recombination time upon the density of *e-h* pairs as a result of Eqs. (7a) and (7b) for a purely radiative recombination or simply set to 100 ps and constant for a recombination widely dominated by nonradiative processes. This simplified modeling of recombination processes yields important information: due to the conjunction of bimolecular recombination and of the screening of electric fields, the radiative decay time decreases by 2 orders of magnitude when n goes from 10^{12} to 10^{13} cm^{-2}.

We present, in Figs. 10(a) and 10(b), the *e-h* pair densities injected in the well versus the excitation density calculated by using Eq. (6) for an excitation energy of 4.1 eV. We have purposely placed this excitation in the "active" region of the spectrum and below the absorption threshold of the $Al_{0.4}Ga_{0.6}N$ barrier. First, these figures show the typical optical power densities necessary to induce interesting effects, i.e., of a few hundred kW/cm^2, which is much smaller than what is required to obtain nonlinear effects with bulk materials (200 MW/cm^2, see Ref. 60). Two extreme hypotheses were considered. First, we have examined for Fig. 10(a) the case where the recombination of *e-h* pairs is dominated by radiative processes. Then, the variation of n is strongly nonlinear due to the competition between (i) the fast increase of the recombination rate with n, according to Eqs. (7a) and (7b) and (ii) the slower increase of the generation rate by enhancement of the absorption coefficient from Eq. (8). This is why the power density needed to inject, for example, 8

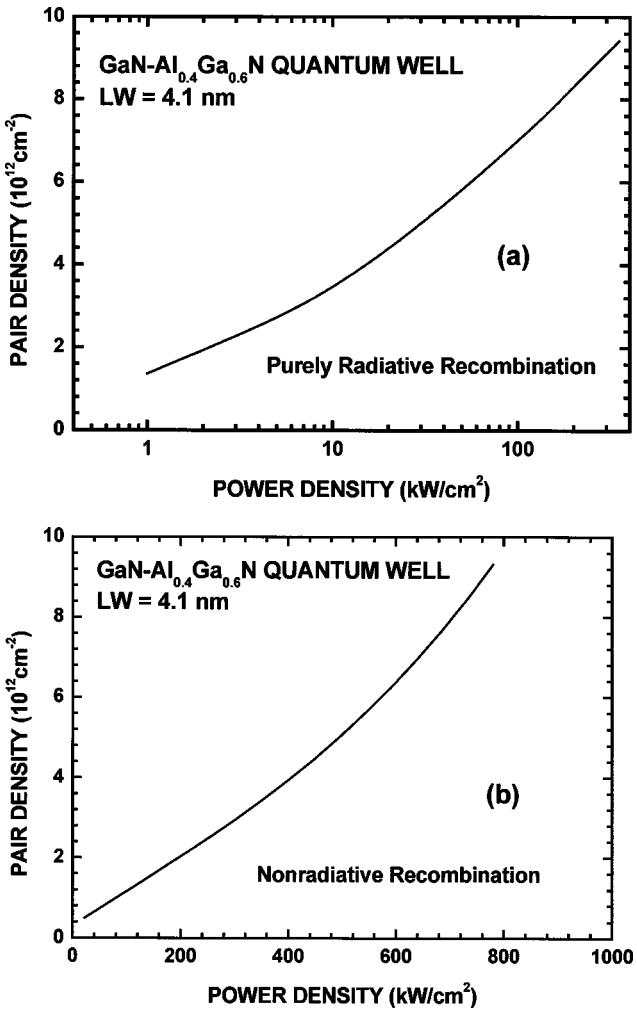

FIG. 10. Dependence of the density of photocreated electron-hole pairs with the incident optical power density, for a 16-ML-wide GaN-$Al_{0.4}Ga_{0.6}N$ single QW and for an excitation photon energy of 4.1 eV. (a) The recombination is dominated by radiative processes; the saturation (or nearly logarithmic increase of n) is induced by the dominant effect of the enhancement of the recombination rate with excitation. (b) The power densities needed for the same pair densities are larger than in case (a), but there is no saturation effect.

$\times 10^{12}$ pairs/cm^2 is 10 times higher than that needed to obtain 4×10^{12} pairs/cm^2. Second [Fig. 10(b)], we have considered the case where the dominant process is the nonradiative recombination with a short nonradiative lifetime (100 ps) independent of n. The result is that slightly larger power densities are needed to produce carrier densities of a few times 10^{12} cm^{-2}, but still remaining in the range lower than 1 MW cm^{-2}.

Of course, the power densities shown in Fig. 10 are scaled by the decay times. If the nonradiative decay time is divided by 10, the power density is multiplied by this factor. On the other hand, for purely radiative recombination, such as that, for GaN/AlN quantum boxes at room temperature,[21] we can benefit from extremely large decay times (over tens of microseconds), thus reducing dramatically the required optical power densities.

To be complete in the discussion of other effects that we did not include in this paper, we should mention thermal effects, i.e., the expected increase of the effective temperature of the system due to the importance of phonon-assisted relaxation processes. We believe that this mechanism can result in a slight redshifting of the spectra that we have calculated and also in the increasing of nonradiative recombination rates for very high excitations. Nevertheless, the effects predicted above, though modified, should be preserved, and they demand to be tested by appropriate experiments on carefully designed samples.

CONCLUSION

We have examined, by using envelope-function calculations, the original nonlinear optical properties induced by high populations of *e-h* pairs in low-dimensional systems based on wurtzite group-III nitride semiconductors. In addition to the straightforward blueshift of the ground-state emission, we have found clear possibilities of self-induced photoabsorption. We have explained why these materials can exhibit such effects that could not be obtained with more familiar semiconductor systems and why they are really promising in terms of flexibility. We have identified the limiting factors for these nonlinear properties and we have estimated the optical power densities required to produce them.

We believe that this theoretical work opens the way for a new type of ''band-gap engineering,'' accounting for the large electric fields in these low-dimensional systems. We believe, too, that this work will lead to interesting experimental research on properties that have not yet been investigated.

ACKNOWLEDGMENTS

S. Kalliakos acknowledges the financial support provided through the European Community's Human Potential Program under Contract No. HPRN-CT-1999-00132, CLERMONT. We also acknowledge support of the French Ministry of Education, Research and Technology within the BOQUANI, NANILUB, and INTRANIT Research Programs.

[1] W. Franz, Z. Naturforsch. A **13A**, 484 (1958).
[2] L. V. Keldysh, Zh. Eksp. Teor. Fiz. **34**, 1138 (1958).
[3] D. A. B. Miller, D. S. Chemla, T. C. Damen, A. C. Gossard, W. Wiegmann, T. H. Wood, and C. A. Burrus, Phys. Rev. Lett. **53**, 2173 (1984).
[4] S. L. Chuang, S. Schmitt-Rink, D. A. B. Miller, and D. S. Chemla, Phys. Rev. B **43**, 1500 (1991).
[5] E. X. Ping and H. X. Jiang, Phys. Rev. B **47**, 2101 (1993).
[6] P. Boring, B. Gil, and K. J. Moore, Phys. Rev. Lett. **71**, 1875 (1993).
[7] D. C. Reynolds, D. C. Look, and B. Jogai, J. Appl. Phys. **88**, 5760 (2000).
[8] S. Fafard, E. Fortin, and J. L. Merz, Phys. Rev. B **48**, 11 062 (1993).
[9] D. L. Smith and C. Mailhiot, Phys. Rev. Lett. **58**, 1264 (1987).
[10] A. N. Cartwright, D. S. McCallum, T. F. Boggess, A. L. Smirl, T. S. Moise, L. J. Guido, R. C. Barker, and B. S. Wherrett, J. Appl. Phys. **73**, 7767 (1993).
[11] M. Livingstone, I. Galbraith, and B. S. Wherett, Appl. Phys. Lett. **65**, 2771 (1994).
[12] X. R. Huang, D. R. Harken, A. N. Cartwright, A. L. Smirl, J. L. Sanchez-Rojas, A. Sacedon, E. Calleja, and E. Muñoz, Appl. Phys. Lett. **67**, 950 (1995).
[13] S. Nakamura, M. Senoh, A. Nagahama, N. Iwasa, T. Yamada, T. Matsushita, and H. Kiyoku, Appl. Phys. Lett. **70**, 2753 (1997).
[14] F. Bernardini, V. Fiorentini, and D. Vanderbilt, Phys. Rev. B **56**, R10024 (1997).
[15] F. Bernardini, V. Fiorentini, and D. Vanderbilt, Phys. Rev. Lett. **79**, 3958 (1997).
[16] F. Bernardini and V. Fiorentini, Phys. Rev. B **57**, R9427 (1998).
[17] Jin Seo Im, H. Kollmer, J. Off, A. Sohmer, F. Scholz, and A. Hangleiter, Phys. Rev. B **57**, R9435 (1998).
[18] M. Leroux, N. Grandjean, M. Laügt, J. Massies, B. Gil, P. Lefebvre, and P. Bigenwald, Phys. Rev. B **58**, R13 371 (1998).
[19] P. Lefebvre, J. Allègre, B. Gil, H. Mathieu, N. Grandjean, M. Leroux, J. Massies, and P. Bigenwald, Phys. Rev. B **59**, 15 363 (1999).
[20] P. Lefebvre, A. Morel, M. Gallart, T. Taliercio, J. Allègre, B. Gil, H. Mathieu, B. Damilano, N. Grandjean, and J. Massies, Appl. Phys. Lett. **78**, 1252 (2001).
[21] B. Damilano, N. Grandjean, F. Semond, J. Massies, and M. Leroux, Appl. Phys. Lett. **75**, 962 (1999).
[22] F. Widmann, J. Simon, B. Daudin, G. Feuillet, J. L. Rouvière, N. T. Pelekanos, and G. Fishman, Phys. Rev. B **58**, R15 989 (1998).
[23] M. B. Nardelli, K. Rapcewicz, and J. Bernholc, Phys. Rev. Lett. **71**, 3135 (1997).
[24] T. Honda, T. Miyamoto, T. Sakaguchi, H. Kawanishi, F. Koyanca, and K. Iga, J. Cryst. Growth **189/190**, 644 (1998).
[25] P. Lefebvre, T. Taliercio, A. Morel, J. Allègre, M. Gallart, B. Gil, H. Mathieu, B. Damilano, N. Grandjean, and J. Massies, Appl. Phys. Lett. **78**, 1538 (2001).
[26] P. Bigenwald, A. Kavokin, B. Gil, and P. Lefebvre, Phys. Rev. B **61**, 15 621 (2000).
[27] G. H. Gainer, Y. H. Kwon, J. B. Lam, S. Bidnyk, A. Kalashyan, J. J. Song, S. C. Choi, and G. M. Yang, Appl. Phys. Lett. **78**, 3890 (2001).
[28] S. P. Łepkowski, T. Suski, P. Perlin, V. Yu. Ivanov, M. Godlewski, N. Grandjean, and J. Massies, J. Appl. Phys. **91**, 9622 (2002).
[29] F. Della Sala, A. Di Carlo, P. Lugli, F. Bernardini, V. Fiorentini, R. Scholz, and J. Jancu, Appl. Phys. Lett. **74**, 2002 (1999).
[30] E. Kuokstis, J. W. Yang, G. Simin, M. Asif Khan, R. Gaska, and M. S. Shur, Appl. Phys. Lett. **80**, 977 (2002).
[31] A. Reale, A. Di Carlo, P. Lugli, and A. Kavokin, Phys. Status Solidi A **183**, 121 (2001).
[32] A. Vinattieri, D. Alderighi, J. Kudrna, M. Colocci, A. Reale, A. Di Carlo, P. Lugli, F. Semond, N. Grandjean, and J. Massies, Phys. Status Solidi A **190**, 87 (2002).
[33] A. Reale, G. Massari, A. DiCarlo, and P. Lugli, Phys. Status Solidi A **190**, 81 (2002).

[34] A. Shikanai, T. Deguchi, T. Sota, T. Kuroda, A. Takeuchi, S. Chichibu, and S. Nakamura, Appl. Phys. Lett. **76**, 454 (2000).
[35] W. Chow, M. Kira, and S. W. Koch, Phys. Rev. B **60**, 1947 (1999).
[36] S. Heppel, A. Hangleiter, S. Bader, G. Brüderl, A. Weimar, V. Kümmler, A. Lell, V. Härle, J. Off, B. Kuhn, and F. Scholz, Phys. Status Solidi A **188**, 59 (2001).
[37] S. H. Park and S.-L. Chuang, Appl. Phys. Lett. **72**, 287 (1998).
[38] S. H. Park and S.-L. Chuang, Appl. Phys. Lett. **76**, 1981 (2000).
[39] B. Gil and A. Alemu, Phys. Rev. B **56**, 12 446 (1997).
[40] B. Gil, in *Semiconductors and Semimetals*, Vol. **57** (Academic, San Diego, 1999), Chap. 6.
[41] M. Kumagai, S. L. Chuang, and H. Ando, Phys. Rev. B **57**, 15 303 (1998).
[42] M. Suzuki, T. Uenoyama, and A. Yanase, Phys. Rev. B **52**, 8132 (1995).
[43] B. Gil, F. Hamdani, and H. Morkoç, Phys. Rev. B **54**, 7678 (1996).
[44] S. H. Park and S. L. Chuang, J. Appl. Phys. **87**, 353 (2000).
[45] G. Bastard, *Wave Mechanics Applied to Semiconductor Heterostructures* (Les Editions de Physique, Les Ulis, France, 1988).
[46] H. Haug and S. Koch, *Quantum Theory of the Optical and Electronic Properties of Semiconductors* (World Scientific, Singapore, 1993).
[47] A. J. Fischer, W. Shan, J. J. Song, Y. C. Chang, R. Horning, and B. Goldenberg, Appl. Phys. Lett. **71**, 1981 (1997).
[48] M. Leroux, N. Grandjean, M. Laügt, J. Massies, B. Gil, P. Lefebvre, and P. Bigenwald, Phys. Rev. B **58**, R13 371 (1998).
[49] P. Lefebvre, M. Gallart, T. Taliercio, B. Gil, J. Allègre, H. Mathieu, N. Grandjean, M. Leroux, J. Massies, and P. Bigenwald, Phys. Status Solidi B **216**, 361 (1999).
[50] B. J. Skromme, H. Zhao, D. Wang, H. S. Kong, M. T. Leonard, G. E. Bulman, and R. J. Molnar, Appl. Phys. Lett. **71**, 829 (1997).
[51] A. S. Baker and S. Illegems, Phys. Rev. B **7**, 53 (1973).
[52] S. L. Chuang and C. S. Chang, Phys. Rev. B **54**, 2491 (1996).
[53] N. Grandjean, J. Massies, and M. Leroux, Appl. Phys. Lett. **74**, 2361 (1999).
[54] M. Shinada and S. Sugano, J. Phys. Soc. Jpn. **21**, 1936 (1966).
[55] P. Lefebvre, P. Christol, and H. Mathieu, Phys. Rev. B **48**, 17 308 (1993).
[56] P. Lefebvre, P. Christol, H. Mathieu, and S. Glutsch, Phys. Rev. B **52**, 5756 (1995).
[57] V. Yu Davydov, A. A. Klochikhin, R. P. Seisyan, V. V. Emtsev, S. V. Ivanov, F. Bechstedt, J. Furthmüller, H. Harima, A. V. Mudryi, J. Aderhold, O. Semchinova, and J. Graul, Phys. Status Solidi B **229**, R1 (2002).
[58] H. P. Maruska and J. J. Tietjen, Appl. Phys. Lett. **15**, 327 (1969).
[59] W. M. Yim, E. J. Stofko, P. J. Zanzucchi, J. I. Pankove, M. Ettenberg, and S. L. Gilbert, J. Appl. Phys. **44**, 292 (1972).
[60] S. Juršenas, G. Kurilčic, G. Tamulaitis, A. Žukauskas, R. Gaska, M. S. Shur, M. A. Khan, and J. W. Yang, Appl. Phys. Lett. **76**, 2388 (2000).